

The AP-3 β Adaptin Mediates the Biogenesis and Function of Lytic Vacuoles in *Arabidopsis*

Elena Feraru,^{a,b,c} Tomasz Paciorek,^c Mugurel I. Feraru,^{a,b,c} Marta Zwiewka,^{a,b} Ruth De Groodt,^{a,b} Riet De Rycke,^b Jürgen Kleine-Vehn,^{a,b,c} and Jiří Friml^{a,b,1}

^aDepartment of Plant Systems Biology, VIB, 9052 Gent, Belgium

^bDepartment of Plant Biotechnology and Genetics, Ghent University, 9052 Gent, Belgium

^cCenter for Plant Molecular Biology (ZMBP), University of Tübingen, 72076 Tübingen, Germany

Plant vacuoles are essential multifunctional organelles largely distinct from similar organelles in other eukaryotes. Embryo protein storage vacuoles and the lytic vacuoles that perform a general degradation function are the best characterized, but little is known about the biogenesis and transition between these vacuolar types. Here, we designed a fluorescent marker-based forward genetic screen in *Arabidopsis thaliana* and identified a protein affected trafficking2 (*pat2*) mutant, whose lytic vacuoles display altered morphology and accumulation of proteins. Unlike other mutants affecting the vacuole, *pat2* is specifically defective in the biogenesis, identity, and function of lytic vacuoles but shows normal sorting of proteins to storage vacuoles. *PAT2* encodes a putative β -subunit of adaptor protein complex 3 (AP-3) that can partially complement the corresponding yeast mutant. Manipulations of the putative AP-3 β adaptin functions suggest a plant-specific role for the evolutionarily conserved AP-3 β in mediating lytic vacuole performance and transition of storage into the lytic vacuoles independently of the main prevacuolar compartment-based trafficking route.

INTRODUCTION

Intracellular protein trafficking is a central feature of eukaryotic cell biology and has been extensively studied in various organisms (Cowles et al., 1997; Dell'Angelica et al., 1999; Surpin et al., 2003). In recent years, protein trafficking in plant cells has been shown to be crucial for many developmental and physiological processes, but fundamental knowledge about various trafficking pathways is still scarce (Robinson et al., 2008). Vacuoles are crucial organelles in plant cells, playing a unique role in development and physiology (Rojo et al., 2001). They are multifunctional organelles, highly variable in their shape, size, number, and luminal content (Marty, 1999; Bassham et al., 2008; Frigerio et al., 2008). Based on their acidity, they can be divided into two main groups: (1) lytic vacuoles that, similarly to the lysosomes found in animals, perform a general degradation function and (2) protein storage vacuoles (PSVs) that mainly store reserve proteins in seeds. Besides the general degradation function, lytic vacuoles are very important for the lytic breakdown of storage proteins during germination, thus providing the germinating seedlings with the necessary nutrients.

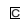
Vacuolar sorting and trafficking are complex processes, and a lot of emphasis has been put on studying trafficking to the lytic

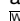
vacuoles and PSVs (Surpin et al., 2003; Shimada et al., 2006; Lee et al., 2007; Sanmartín et al., 2007; Sohn et al., 2007; Ebine et al., 2008; Yamazaki et al., 2008). Protein trafficking from the trans-Golgi network (TGN) toward the vacuoles passes through a heterogeneous group of late endosomes, the prevacuolar compartment/multivesicular bodies (PVC/MVBs) (Marty, 1999). Hence, the PVC/MVBs are considered progenitors of the vacuoles (Marty, 1999).

Adaptor Protein (AP) complexes (AP-1, AP-2, AP-3, and AP-4) have been identified in eukaryotes, such as yeast and mammals, as important regulators of the endocytic and secretory pathways (Boehm and Bonifacino, 2002; Dell'Angelica, 2009). AP-1 is a component of the secretory pathway and functions in the bidirectional trafficking of proteins from the TGN to an endosomal compartment, while AP-2 is found in the endocytic pathway and has a role in the trafficking of proteins from the plasma membrane (PM). It has been shown that both AP-1 and AP-2 bind to the coat protein clathrin during the formation of clathrin-coated vesicles and recognize the sorting signals displayed by the cargos of the vesicles. AP-3 and AP-4 are the most recently identified complexes, and they have been found in association with the TGN/endosomes (Boehm and Bonifacino, 2002; Dell'Angelica, 2009). Unlike AP-1 and AP-2, AP-4 does not interact with clathrin, and the interaction between AP-3 and clathrin is still controversial. Each adaptor protein complex is composed of four subunits called adaptins (Boehm and Bonifacino, 2002). Similar to the other AP complexes, AP-3 is a heterotetrameric complex consisting of two large subunits (δ and β 3), a medium subunit (μ 3), and a small subunit (σ 3) (Boehm and Bonifacino, 2002; Dell'Angelica, 2009). The AP-3 complex has been intensively studied in mammals, flies, and yeast. It has been found that AP-3 sorts proteins from the TGN and/or an endosomal compartment to the lysosome by

¹ Address correspondence to jiri.friml@psb.vib-ugent.be.

The author responsible for distribution of materials integral to the findings presented in this article in accordance with the policy described in the Instructions for Authors (www.plantcell.org) is: Jiří Friml (jiri.friml@psb.vib-ugent.be).

 Some figures in this article are displayed in color online but in black and white in the print edition.

 Online version contains Web-only data.

www.plantcell.org/cgi/doi/10.1105/tpc.110.075424

interacting with their Tyr and dileucine signals and by circumventing the usual PVC/MVB-based trafficking route (Cowles et al., 1997; Stepp et al., 1997; Dell'Angelica et al., 1999; Feng et al., 1999; Kretzschmar et al., 2000).

In the *Arabidopsis thaliana* genome, four putative AP-3 adaptins can be found based on sequence similarity (Bassham et al., 2008), suggesting that the *Arabidopsis* AP-3 complex is represented by single copy genes, contrasting with the mammalian AP-3 complex that has ubiquitously expressed and brain-specific isoforms of most of the AP-3 adaptins (Boehm and Bonifacino, 2002; Bassham et al., 2008; Dell'Angelica, 2009). The function of the AP-3 complex in plants, including *Arabidopsis*, has not yet been definitely elucidated. A loss-of-function mutant in the putative AP-3 μ adaptin has been identified as a suppressor of *zigzag1* (*zig1*), which is defective in the SNARE VTI11, a regulator of vesicle trafficking between the TGN and PVC/vacuole (Surpin et al., 2003; Sanmartín et al., 2007; Niihama et al., 2009). Furthermore, mutants in the putative AP-3 δ and AP-3 β adaptins display similar phenotypes and have the same function (Niihama et al., 2009), providing strong evidence for the existence of a functional AP-3 complex in *Arabidopsis*. It has been also shown that vesicle transport regulator EpsinR2 interacts with the putative δ -subunit of AP-3 and binds to clathrin and phosphatidylinositol 3-phosphate (Lee et al., 2007) as well to VTI12 that has a role in protein trafficking to the PSV (Lee et al., 2007; Sanmartín et al., 2007). Furthermore, TERMINAL FLOWER1 (TFL1), a protein that plays a role in PSV trafficking resides in AP-3 δ positive endosomes (Sohn et al., 2007), indicating that AP-3-dependent endosomes could regulate trafficking to the PSV/vacuoles.

Here, we report the identification and characterization of the putative β -subunit of the AP-3 complex, a novel regulator of vacuolar biogenesis and function in *Arabidopsis*. Deletion of the putative $\beta 3$ adaptin resulted in enhanced vacuolar accumulation of integral PM and soluble proteins and causes aberrant PSV, lytic vacuole, and PVC morphologies. Our analysis also revealed that AP-3 β function is evolutionarily conserved, but in plants, AP-3 β acquired a unique function in regulating vacuolar biogenesis and function, including the transition between storage and lytic vacuolar types.

RESULTS

Identification of protein affected trafficking Mutants

To better characterize the protein trafficking pathways in *Arabidopsis*, we designed a fluorescence imaging-based forward genetic screen. As a tool for the screening to identify novel components of plant intracellular trafficking, we used a well-characterized plant cargo, the auxin efflux carrier PIN1 (Petrásek et al., 2006). PIN1 is an integral membrane protein that undergoes complex, constitutive subcellular dynamics, including nonpolar secretion (Dhonukshe et al., 2008), clathrin-mediated endocytosis (Dhonukshe et al., 2007), GTP exchange factor on ADP-ribosylation factors-dependent polar recycling (Geldner et al., 2001; Kleine-Vehn et al., 2008a), and vacuolar targeting (Abas et al., 2006; Kleine-Vehn et al., 2008b). With this strategy, we aimed to identify novel regulators at different stages of

subcellular protein trafficking. We screened an ethyl methane-sulfonate (EMS)-mutagenized *PIN1_{pro}-PIN1-GFP* (for green fluorescent protein) population using epifluorescent microscopy for seedlings displaying aberrant PIN1-GFP distribution in the root. From 1500 M1 families, we identified several *protein affected trafficking* (*pat*) mutants defining three independent loci.

The *pat2* Mutant Shows Strong Intracellular Accumulation of Proteins

We further analyzed in detail the *pat2* mutant showing strong accumulation of PIN1-GFP in the root cells. Whereas control PIN1-GFP plants displayed preferential PM localization at the basal (lower) side of stele cells (Benková et al., 2003), *pat2* mutants showed additionally strong intracellular accumulation of PIN1-GFP (Figures 1A and 1B; see Supplemental Figures 1A to 1D, 2A, and 2B online). Also, other polar and nonpolar integral PM proteins, such as PIN7-GFP (Bilou et al., 2005), PIN1-GFP expressed under the PIN2 promoter (Wiśniewska et al., 2006), PIN2-GFP (Xu and Scheres, 2005), and the aquaporin PIP2a (Cutler et al., 2000) as well as soluble proteins, such as aleurain (di Sansebastiano et al., 2001), accumulated intracellularly in the different cell types of the *pat2* mutant (Figures 1C and 1D; see Supplemental Figures 1E, 2E, 2F, 2I, 2J, 2M, 2N, 2Q, and 2R online). These results show that PM-localized and soluble proteins have defective subcellular distribution and accumulate in the *pat2* mutant.

Notably, despite massive subcellular accumulation of different cargos, the *pat2* mutants showed an almost normal morphology when grown under widely used *Arabidopsis* growth conditions (see Supplemental Figures 3A, 3B, and 3E online), with the exception of a defect in the shoot gravitropic response (Figure 1F; see Supplemental Figures 3C and 3D online). Only when grown on medium lacking sucrose, the mutant seedlings showed shorter roots and formed less lateral roots, and some of them displayed arrested growth (Figures 1E and 1G; see Supplemental Figures 3F and 3G online). The percentage of arrested seedlings was correlated with the age of the seeds (10.5% for 2-month-old *pat2-1* and 44.9% for 9-month-old *pat2-1*), and after longer storage, the mutant seeds showed dramatically reduced germination capacity (see Supplemental Figure 3G online). Some of these phenotypes are reminiscent of mutants affected in vacuolar function, including the PSV (Kato et al., 2002; Kleine-Vehn et al., 2008b; Silady et al., 2008), and the absence of strong morphological defects and/or auxin-related phenotypes in *pat2* mutants indicates that the intracellular accumulations represent a pool of nonactive proteins. Accordingly, the PM localization and abundance of PIN1-GFP at the basal PM, its secretion, and constitutive endocytosis as well as recycling were not altered in *pat2* mutant roots (Figure 1H; see Supplemental Figure 4 online). Thus, our PIN1-GFP marker-based screen identified the *pat2* mutant, which is defective in intracellular protein distribution; this would be hardly possible by a conventional screen due to the lack of obvious morphological phenotypes. The *pat2* mutation appears to specifically cause intracellular accumulation of proteins but does not visibly affect major secretory and endocytic trafficking routes.

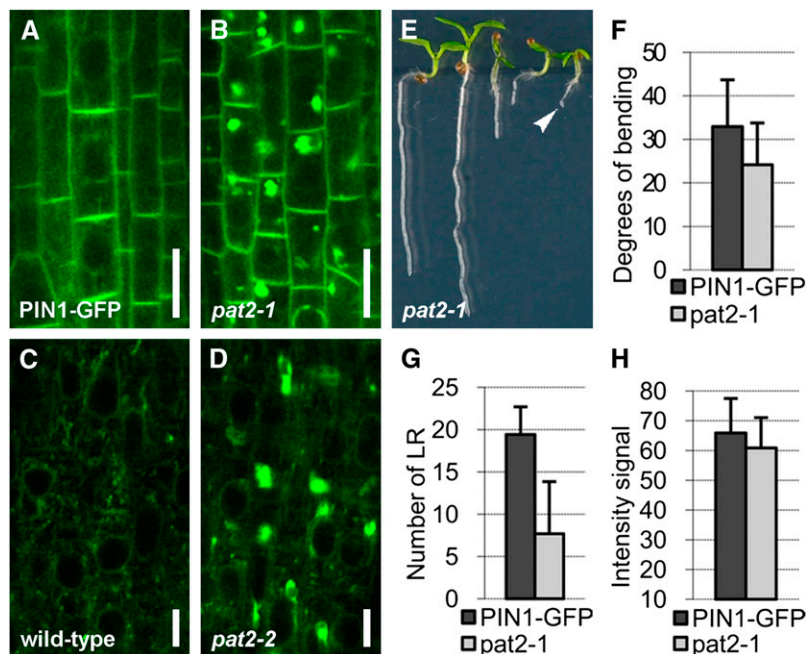


Figure 1. The *pat2* Mutant Displays Ectopic Intracellular Protein Accumulation.

(A) to (D) Both PIN1-GFP ([A] and [B]) and aleurain-GFP ([C] and [D]) accumulate intracellularly in *pat2-1* (B) or *pat2-2* (D) root cells compared with control ([A] and [C]).

(E) Some *pat2-1* seedlings arrest on medium without sucrose (arrowhead). Note both the arrested and wild-type-looking seedlings in a population of 7-d-old *pat2-1*.

(F) and (G) Hypocotyl gravitropic response ($n = 75$) (F) and lateral root formation ($n = 75$) (G) are affected in *pat2-1*.

(H) Intensity of PIN1-GFP signal at the PM of root stele cells is not obviously affected in *pat2-1* ($n = 110$).

Error bars represent SD. Bars = 10 μm in (A) and (B) and 5 μm in (C) and (D).

PAT2 Encodes a Functional Putative β -Subunit of the AP-3 Complex

To molecularly characterize the *pat2* mutation, we mapped it with ~ 1000 chromosomes from the F2 progeny derived from crosses of *pat2-1* with the Landsberg *erecta* wild type. We found a premature stop codon (Figure 2A) in the gene coding for an adaptin family protein similar to the $\beta 3A$ subunit of the mammalian AP-3 complex (Dell'Angelica et al., 1999). The expression of the AP-3 β transcript, as revealed by RT-PCR, was reduced in *pat2-1* and totally absent in *pat2-2*, a T-DNA allele that we isolated (Figure 2B). Recessive and loss-of-function *pat2-1* and *pat2-2* showed comparable subcellular phenotypes (see Supplemental Figures 1A to 1D online) that were complemented by expression of AP-3 β_{pro} :AP-3 β -GFP (Figures 2C to 2F). Furthermore, AP-3 β_{pro} :AP-3 β -GFP rescued both the arrested phenotype and the defective hypocotyl response of the *pat2-1* mutant (see Supplemental Figure 5 online). Collectively, these data show that the defects in protein trafficking in the *pat2* mutants are due to the mutation in the gene coding for a putative AP-3 β adaptin.

To test whether PAT2 encodes an AP-3 β with evolutionarily conserved function, we made use of the yeast *Saccharomyces cerevisiae* AP-3 β -deficient mutant (*apl6 Δ*) that is defective in the Alkaline phosphatase (ALP) sorting to the vacuole (Cowles et al., 1997). PAT2 cDNA partially restored the ALP-GFP localization to

the vacuole in the *apl6 Δ* mutant background (Figures 2G to 2I), confirming that PAT2 encodes the functional AP-3 β adaptin. It also shows that the function of AP-3 β is evolutionarily conserved between yeast and higher plants.

AP-3 β Adaptin Is a Component of a Brefeldin A- and Wortmannin-Insensitive Pathway

To analyze AP-3 β function in *Arabidopsis*, we examined its expression and subcellular localization. Transgenic AP-3 β_{pro} :GFP-GUS (for β -glucuronidase) lines showed ubiquitous expression throughout the embryonic and postembryonic development (Figures 3A to 3C; see Supplemental Figure 6 online) as confirmed by public transcriptomics data (<http://bbc.botany.utoronto.ca>). Functional AP-3 β_{pro} :AP-3 β -GFP (Figures 2C to 2E) revealed that AP-3 β localized mainly to the cytosol as expected for a soluble adaptor protein, but it also showed weak association with endomembrane structures (Figures 3D to 3F). In the root meristematic zone, the AP-3 β -GFP endomembrane structures were absent or very few and extremely small, while they became more prominent and enlarged in the elongation and differentiated zones (Figures 3E and 3F), presumably reflecting a compartment maturation process. When overexpressed, AP-3 β -GFP became more strongly associated with the endomembranes (Figure 3G). To address the identity of the AP-3 β -positive endomembranes, we used inhibitor

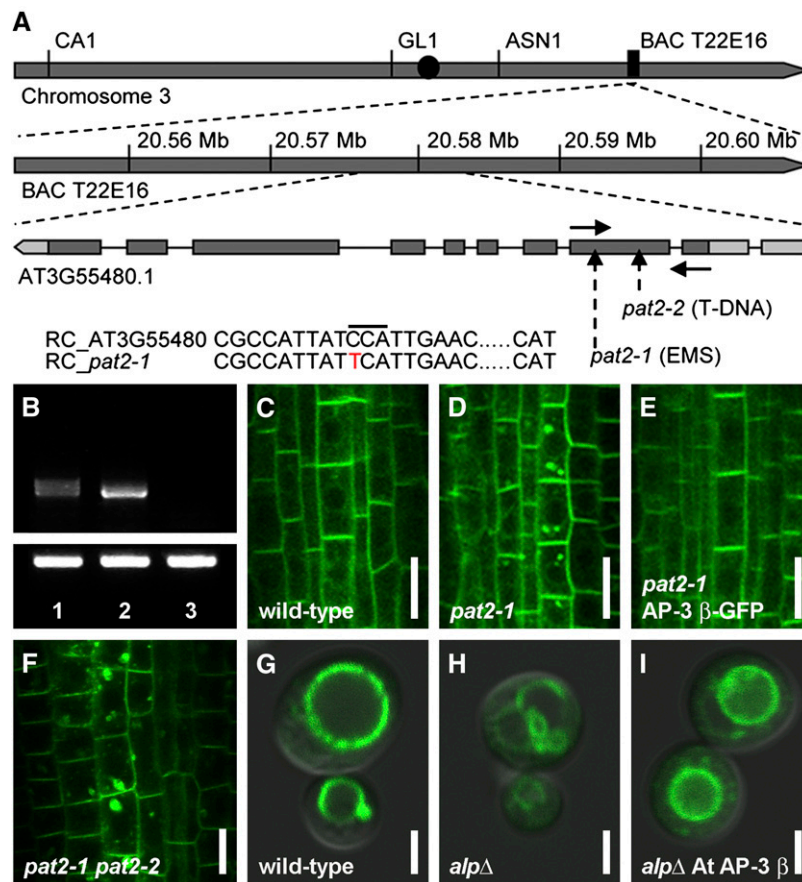


Figure 2. *PAT2* Encodes a Putative AP-3 β Adaptin, a Protein with Conserved Function among Eukaryotes.

(A) Scheme of putative AP-3 β locus and organization. The positions of *pat2* alleles (dash arrows), the forward and reverse primers used for RT-PCR (solid arrows), and the point mutation (red letter) are depicted.

(B) Expression of the AP-3 β transcript detected by RT-PCR is shown for *pat2-1* (1), the wild type (2), and *pat2-2* (3). Tubulin is shown in the bottom panel.

(C) to (E) Complementation test. Localization of PIN1-GFP in wild-type **(C)**, *pat2-1* **(D)**, and recovered in *pat2-1* transformed with AP-3 β_{pro} :AP-3 β -GFP **(E)**.

(F) Allelic test showing PIN1-GFP accumulation in *pat2-1 pat2-2* F1 seedlings.

(G) to (I) ALP-GFP localization in wild-type yeast **(G)**, *alp6 Δ* mutant **(H)**, and *alp6 Δ* transformed with *Arabidopsis* AP-3 β **(I)**.

RC, reverse complement. Bars = 10 μ m in **(C) to (F)** and 2 μ m in **(G) to (I)**.

treatments and subcellular markers. In *Arabidopsis*, brefeldin A (BFA) treatment typically leads to accumulation of cargo, including PIN1 into the so-called BFA compartment encompassing aggregation of early endosomes/TGN and recycling endosomes that get surrounded by the Golgi apparatus (GA) (Geldner et al., 2001; Grebe et al., 2003; Dettmer et al., 2006; Robinson et al., 2008). The AP-3 β -positive endomembranes were not sensitive to a 1-h treatment with 50 μ M BFA, revealing that AP-3 β does not localize to recycling endosomes, early endosomes/TGN, or GA (Figure 3H; see Supplemental Figures 7A and 7B online). Nonetheless, we observed a sporadic occurrence of AP-3 β in the vicinity of the BFA compartment (Figure 3H). AP-3 β compartments were also not altered after a 2-h treatment with 33 μ M wortmannin (see Supplemental Figure 7C online). Wortmannin is an inhibitor of the phosphatidylinositol-3-kinase and, to a lesser extent, of the PI4-

kinase activity that causes swelling of PVCs (Tse et al., 2004; Haas et al., 2007). This result suggests that AP-3 β does not localize to PVC compartments. Furthermore, AP-3 β -GFP structures did not show a pronounced colocalization with known GA, TGN, or PVC markers, such as SEC21, SYP61, and SYP21 (Figures 3I to 3K; see Supplemental Figures 7D to 7F online). These data suggest that AP-3 β shows cytosolic localization and weak association with a thus far uncharacterized endomembrane compartment that is not a part of the BFA- and wortmannin-sensitive pathways.

***pat2* Ectopically Accumulates Cargo in Vacuole-Like Compartments**

Next, we addressed how the loss of AP-3 β function in *pat2* mutants leads to ectopic protein accumulation. A 1-h treatment

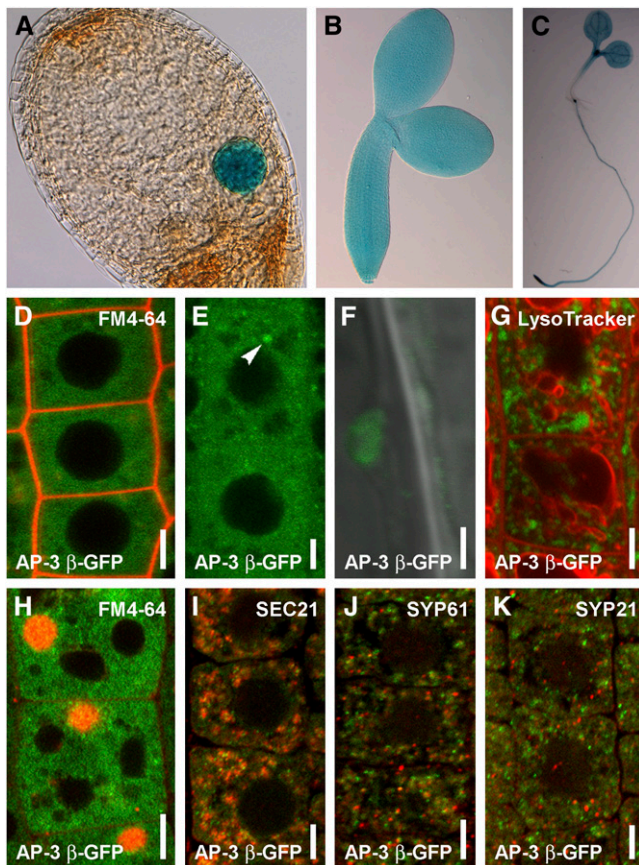


Figure 3. Ubiquitously Expressed PAT2/AP-3 β Is Localized by a BFA- and Wortmannin-Independent Pathway in *Arabidopsis*.

(A) to (C) AP-3 β_{pro} :GUS-GFP expression in embryos [(A) and (B)] and in a 7-d-old seedling (C).

(D) to (F) Pronounced cytosolic localization of AP-3 β -GFP (green) in wild-type root meristematic cells stained shortly by FM4-64 (2 μ M) (red) (D). Small AP-3 β -GFP structures can be observed in the epidermal and cortex cells of the upper meristematic zone (arrowhead) (E). AP-3 β -GFP structures look vesiculated in the elongation zone (F).

(G) GFP (green) in $35S_{pro}$:AP-3 β -GFP root cells does not show colocalization with LysoTracker red (2 μ M, 1 h) (red).

(H) Treatment of 1 h BFA (50 μ M) on AP-3 β_{pro} :AP-3 β -GFP (green) stained with FM4-64 (4 μ M) (red).

(I) to (K) Immunolocalizations show that AP-3 β -GFP structures (green) only randomly associate with SEC21 (I), SYP61 (J), and SYP21 (K). Markers depicted in red.

Bars = 5 μ m (D), (E), and (G) to (K) and 2 μ m in (F).

with 50 μ M BFA of cells stained with the membrane-bound endocytic tracer FM4-64 showed that the ectopically accumulating PIN1-GFP in *pat2* does not localize to the BFA compartment (Figures 4A and 4B). Hence, protein accumulation in the *pat2* mutant does not result from defects in secretion, endocytosis, and/or recycling (see Supplemental Figure 4 online). Accordingly, PIN1-GFP did not ectopically accumulate in the related compartments, including GA and early endosomes/TGN of *pat2-2*, and markers that label these compartments, such as VHA-a1-GFP (Dettmer et al., 2006), VTI12-YFP (for yellow fluorescent protein;

Geldner et al., 2009), and N-ST-YFP (Grebe et al., 2003), showed normal localization in *pat2* mutants (see Supplemental Figure 8 online). These data show that secretory and early endosomal compartments are not the place of ectopic protein accumulation.

We used FM4-64 to follow the late endocytic compartments, including vacuoles in *pat2*, because prolonged FM4-64 treatments also label the tonoplast (Ueda et al., 2001; Kleine-Vehn et al., 2008b). Labeling with 4 μ M FM4-64 for 3.5 h clearly colocalized with the ectopic PIN1-GFP signal in *pat2-1* cells (Figure 4C). Similarly, after 1 h, 2 μ M of the fluorescent acidotropic probe, LysoTracker red, which labels acidic vacuoles (Laxmi et al., 2008), accumulated in *pat2-1* in the same structures as PIN1-GFP (Figures 4D and 4E). To confirm that proteins accumulate ectopically in *pat2* in vacuole-like compartments and investigate a possible decrease in the actual lytic degradation rate, we used the known property of GFP that is more stable in lytic vacuoles in the dark (Tamura et al., 2003; Kleine-Vehn et al., 2008b; Laxmi et al., 2008). Dark treatment led to clearly enhanced signal intensity of the ectopic, intracellular PIN1-GFP (see Supplemental Figures 2A to 2D online). The same effect was observed for PIN1-GFP expressed under the PIN2 promoter, PIN7-GFP, PIN2-GFP, and PIP2-GFP (Figures 4F and 4G; see Supplemental Figures 2E to 2T and 9 online). These findings show that *pat2* mutant cells accumulate different proteins in vacuole-type compartments and suggest that this is a consequence of the defect in the vacuolar lytic degradation.

pat2 Is Defective in the Morphology, Function, and PVC-Dependent Biogenesis of the Lytic Vacuoles

To study how the AP-3 β function can regulate the vacuolar accumulation of proteins, we analyzed the vacuole morphology in *pat2* mutants. Labeling with 4 μ M FM4-64 for 4-h, as well as the localization of the tonoplast markers, such as SYP22-YFP (Robert et al., 2008) and EGFP- δ TIP (Cutler et al., 2000), revealed dramatic morphological alterations of the vacuoles that involved ectopic endomembrane inclusions into the *pat2* vacuolar lumen (Figures 4H to 4K; see Supplemental Figures 9 and 10A to 10C online). Analysis of the ultrastructure by transmission electron microscopy further substantiated the abnormal vacuole morphology in *pat2* (Figures 4L to 4R; see Supplemental Figures 10D and 10E online). Contrasting with the control endodermal cells that were occupied by several small and fusing vacuoles, in the *pat2* mutant, most of the cells were occupied by a singular abnormal-shaped vacuoles (see Supplemental Figures 10D and 10E online). The existence of aberrant-shaped vacuoles with various multilayered endomembrane enclosures shows that the biogenesis of the lytic vacuole is severely altered in *pat2* mutants. Furthermore, immunogold labeling showed enhanced accumulation of PIN1-GFP in the multilayered endomembranes, confirming the reduced degradation of proteins in the aberrant *pat2-1* vacuoles (Figure 4O).

Next, we analyzed the identity of the lytic vacuoles in *pat2* mutants. As acidification of vacuoles is a key feature in lytic vacuole differentiation (Frigerio et al., 2008), the pH indicator 2',7'-b/s(2-carboxyethyl)-5(6)-carboxyfluorescein (BCECF), which accumulates in the acidic organelles (Swanson and Jones, 1996), as well as LysoTracker red, were used to assess lytic

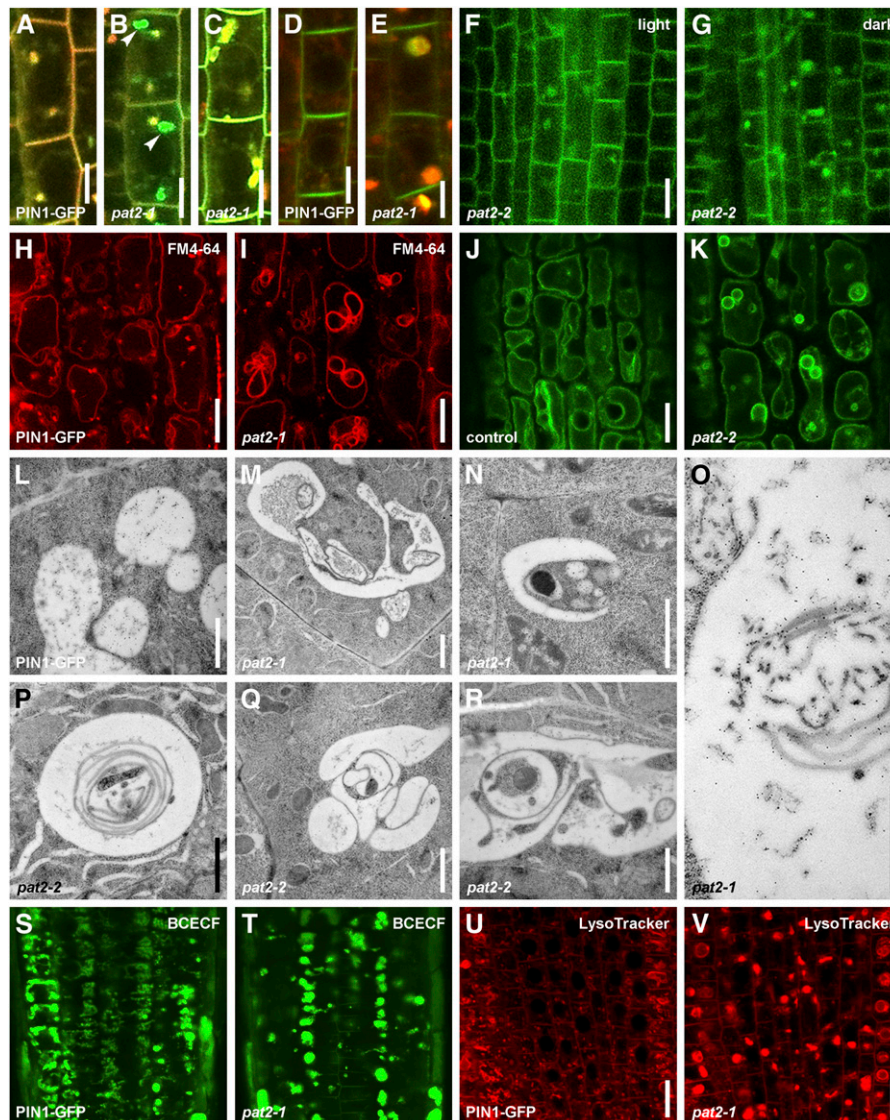


Figure 4. Lytic Vacuole Morphology, Biogenesis, and Lytic Degradation Are Impaired in the *pat2* Mutant.

(A) and (B) BFA (50 μ M, 1 h) treatment on FM4-64 (4 μ M) stained control (A) and *pat2-1* (B) stele cells. See the complete colocalization of FM4-64 (red) and PIN1-GFP (green) in BFA compartments (yellow) of the control (A). Note that PIN1-GFP aggregations in *pat2-1* (green; arrowheads) are distinct from BFA compartments (yellow) (B).

(C) FM4-64 (4 μ M, 3.5 h) stains PIN1-GFP-containing compartments in the stele cells of *pat2-1* (yellow).

(D) and (E) LysoTracker red (2 μ M; 1 h) vacuolar accumulation colocalizes with PIN1-GFP aggregations in *pat2-1* roots (yellow) (E) compared with control (D).

(F) and (G) PIP2a-GFP aggregations in *pat2-2* get enhanced after 2.5 h of dark treatment (G) compared with light (F).

(H) to (V) *pat2* lytic vacuoles show altered morphology. FM4-64 (4 μ M; 4 h) staining of the tonoplast in control (H) and *pat2-1* (I). The localization of SYP22-YFP in control (J) and *pat2-2* (K) epidermal cells. Electron micrographs for control (L), *pat2-1* (M) to (O), and *pat2-2* (P) to (R) root endodermal cells. Immunogold labeling shows accumulation of PIN1-GFP on the multilayered endomembranes present in the *pat2-1* vacuoles (O). BCECF (10 μ M; 40 min) accumulation in control (S) and *pat2-1* mutant (T) and LysoTracker red (2 μ M; 1 h) in control (U) and *pat2-1* (V).

Bars = 5 μ m in (A) to (E), 10 μ m in (F) to (K), 1 μ m in (L) to (R), and 20 μ m in (U) and (V).

vacuole differentiation. The *pat2* mutants showed abnormal accumulation of BCECF and LysoTracker red (Figures 4S to 4V; see Supplemental Figure 10F online). BCECF dye stained in *pat2-1* cells with either enhanced or reduced labeling but also revealed that the *pat2* mutant often lacked the tubular extensions

that could be observed in the control cells (Figures 4S and 4T; see Supplemental Figure 10F online), which might resemble tubular provacuoles (Marty, 1999). These findings suggest defects in biogenesis and maturation of *pat2* vacuoles and prompted us to analyze the PVC-dependent lytic vacuole biogenesis. The

vacuole-like structures in *pat2* were affected by wortmannin (see Supplemental Figures 10G and 10H online), suggesting that *pat2* vacuoles have changed identity.

PVC markers, such as GFP-RABF2b, RABF1-GFP (Jaillais et al., 2006), and SYP22-YFP, showed altered morphology in the *pat2-2* mutant (Figures 5A to 5D). GFP-RABF2b-labeled endomembranes appeared aberrant shaped and strongly vacuolated in the *pat2-2* stele cells (Figures 5A and 5B). Notably, the PVC phenotypes of *pat2* mutants could be phenocopied by only 1 h of 33 μ M wortmannin on GFP-RABF2b and SYP22-YFP (Figures 5E to 5L). These results reveal that the vacuolar structures in *pat2* cells have characteristics of both vacuoles, such as typical overall morphology and presence of vacuolar markers as well as of PVCs, such as wortmannin sensitivity and presence of PVC markers. These structures might represent a mixed identity compartment as supported also by electron microscopy analysis (see Figures 4L to 4R). This affects the overall performance of the vacuoles, hence leading to a defect in the lytic degradation of proteins. Altogether, our data suggest that the PVC-dependent biogenesis of lytic vacuoles is affected in the *pat2* mutants, leading to altered morphology and function of the vacuole.

***pat2* Is Defective in Transition from Storage to Lytic Vacuole**

Several mutants show defects in the late steps of the endocytic pathway that interfere with the proper cargo delivery to storage

and/or lytic vacuoles (Shimada et al., 2006; Kleine-Vehn et al., 2008b; Ebine et al., 2008). The developmental arrest of the *pat2* mutants on medium without an energy source (Figure 1E; see Supplemental Figure 3G online) is typical for mutants with defects in storage vacuoles (Shimada et al., 2006; Kleine-Vehn et al., 2008b; Silady et al., 2008). Accordingly, the morphology of *pat2* PSVs is defective, and the *pat2* embryo cells display abnormally sized and spherical-shaped PSVs (Figures 6A, 6B, and 6G; see Supplemental Figure 11 online). Ultrastructure examination by transmission electron microscopy confirmed the altered morphology of PSVs in *pat2* mutants (Figures 6C to 6F).

Furthermore, we investigated whether the observed defects in PSV morphology were associated with missorting of storage proteins. Previous studies have revealed that reserve proteins, such as albumins and globulins, accumulate at high amounts in seed PSVs, and various mutants defective in PSV display ectopic sorting of these proteins to the extracellular space (Shimada et al., 2006; Sanmartín et al., 2007; Ebine et al., 2008). However, we could not detect any extracellular accumulation of 2S albumin and 12S globulin storage protein precursors in the dry seeds of *pat2* (Figures 6H to 6J). This finding shows that, despite detectable morphological defects, the sorting and delivery of storage proteins to *pat2* PSVs are unaffected and suggests that the development of the PSVs might be disrupted in the *pat2* mutants.

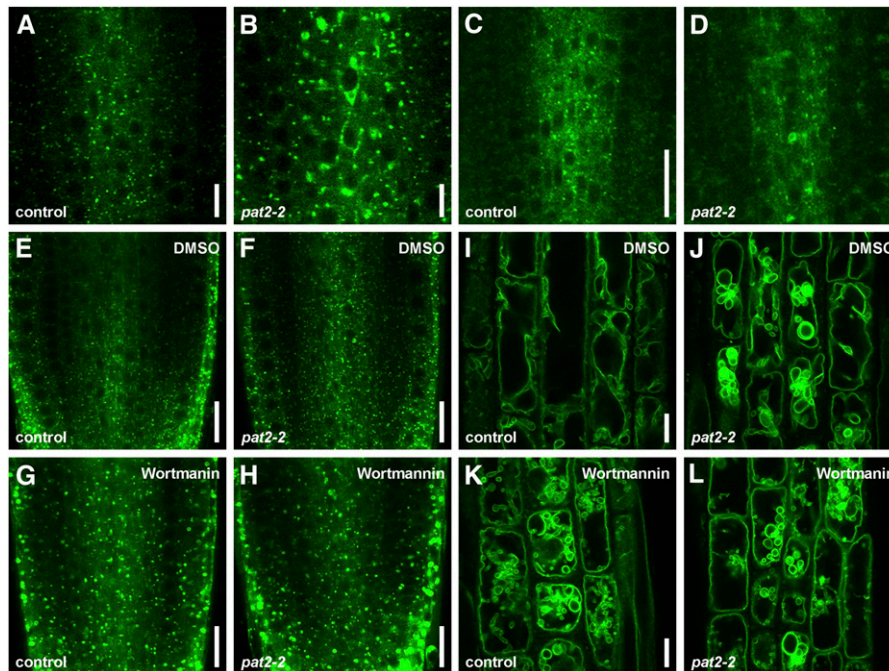


Figure 5. *pat2* Is Defective in PVC-Dependent Lytic Vacuole Biogenesis.

(A) to (D) Localization of GFP-RABF2b (A) and (B) and RABF1-GFP (C) and (D) reveals strong vacuolation of the late endosomes/PVCs in *pat2-2* (B) and (D) compared with the control (A) and (C).

(E) to (L) GFP-RABF2b and SYP22-YFP endosome morphology in the control (E) and (I) and *pat2-2* (F) and (J) treated with DMSO and in the control (G) and (K) and *pat2-2* (H) and (L) after 1 h wortmannin (33 μ M) treatment. Note the similarity between the wortmannin and *pat2* mutation effects on GFP-RABF2b and SYP22-YFP endosomes.

Bars = 10 μ m in (A), (B), and (I) to (L) and 20 μ m in (C) to (H).

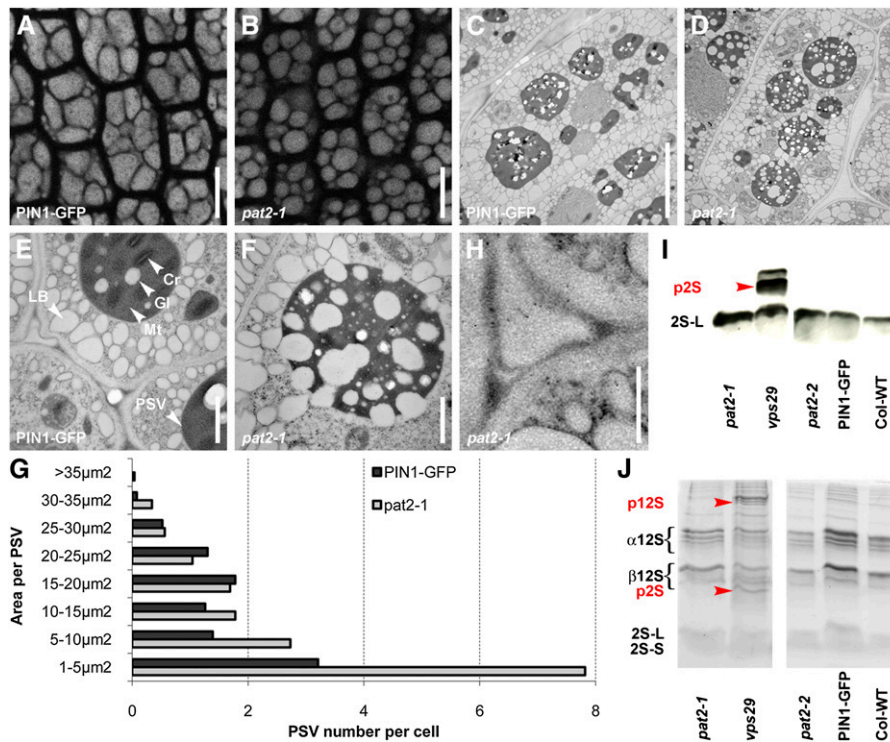


Figure 6. *pat2* Is Not Defective in the Trafficking of Storage Proteins to PSV.

(A) to (G) PSV autofluorescence (imaged immediately after peeling off the seed coat of the dry seeds) in root cells of control (A) and *pat2-1* (B). Electron micrographs of control (C) and (E) and *pat2-1* embryo root cells (D) and (F). Histogram evaluating the morphology of PSVs ($n = 24$ cells) (G).

(H) to (J) Immunogold labeling shows no accumulation of 2S albumin in the intercellular space of *pat2-1* (H). Immunoblot (I) and SDS-PAGE (J) reveal no accumulation of 2S albumin and 12S globulin precursors in *pat2* mutants, but they accumulate in the *vps29*, a mutant known to mis-sort the reserve proteins.

Cr, crystalloid; Gl, globoid; Mt, matrix; p2S, 2S precursors; p12S, 12S precursors. Bars = 10 μm in (A) and (B), 5 μm in (C) and (D), 1 μm in (E) and (F), and 0.5 μm in (H).

[See online article for color version of this figure.]

As the sorting of storage proteins to the storage vacuoles in *pat2* did not appear to be defective and the lytic *pat2* vacuoles have morphological and functional features of PSVs (accumulation of proteins instead of their degradation; defects in acidification), we tested the transition between PSVs and the lytic vacuoles in the *pat2-2* mutant. The time course of LysoTracker red accumulation showed altered acidification patterns of *pat2-2* PSVs (see Supplemental Figure 12 online). Furthermore, whereas most of the control PSVs broke during their development into a network of tubular extensions resembling probably provacuoles (Marty, 1999), *pat2-2* PSVs did not show this transition and displayed an abnormal morphology (Figures 7A to 7H). Surprisingly, the degradation of the storage proteins, such as 2S albumin, was not obviously affected in the *pat2-1* mutant. We could not observe significant defects in the decrease of 2S amount within 4 d following the germination (Figures 7I to 7L; see Supplemental Figure 13 online). These findings show that *pat2* is defective in the conversion of the storage into lytic vacuoles and in the biogenesis of lytic vacuoles. However, the breakdown of the storage proteins still occurs during the germination, but the availability of the resulted energy is limited to *pat2* mutant.

DISCUSSION

A Fluorescence Imaging–Based Forward Genetic Screen Identifies Novel Regulators of Protein Trafficking

To identify novel regulators of protein trafficking pathways in *Arabidopsis*, we designed a fluorescence imaging–based forward genetic screen with the potential to identify mutants that would be difficult to identify by conventional screens based on morphological phenotypes. We screened an EMS-mutagenized *PIN1_{pro}:PIN1-GFP* population by epifluorescent microscopy to search for seedlings with changed intracellular distribution of PIN1-GFP in the primary root. We identified several *pat* mutants defining three independent loci.

The identified *pat* mutants do not show strong morphological phenotypes but still displayed clearly discernible defects in protein trafficking, as exemplified by PIN1-GFP. *pat2* is a recessive loss-of-function mutant defective in a putative β -subunit of the AP-3 complex, and other alleles identified in indexed insertion mutant libraries show similar morphological and cellular phenotypes. The AP-3 complex plays a role in protein trafficking

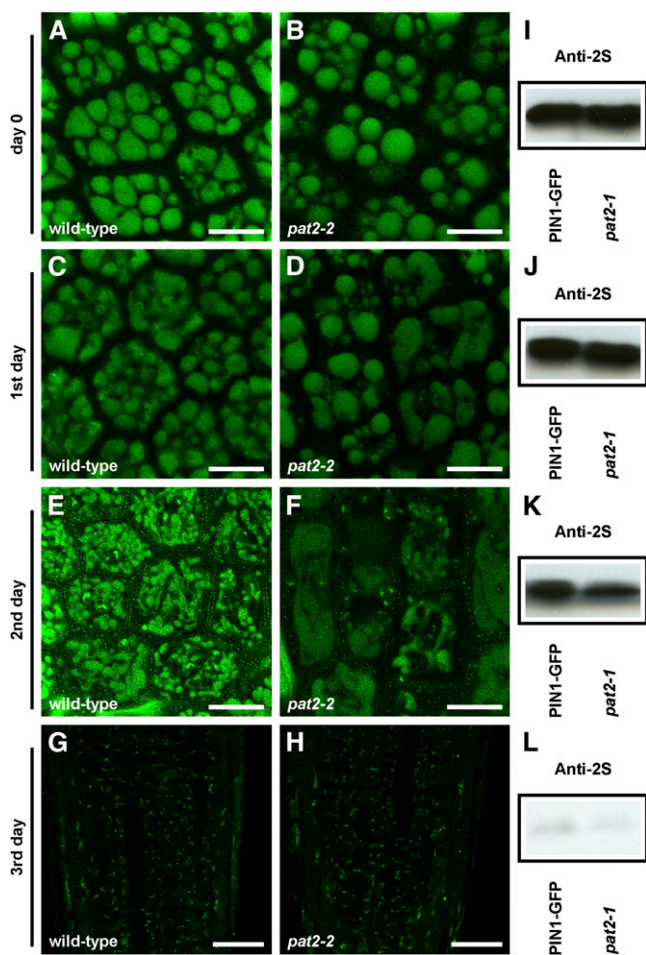


Figure 7. *pat2* Is Defective in the Transition between PSV and Lytic Vacuole.

(A) to (H) Live imaging of the PSV autofluorescence in the wild-type (A), C, E, and G) and *pat2-2* (B, D, F, and H) embryos grown on medium without sucrose (long day, 18°C) and imaged immediately after stratification (A and B), 1 d later (C and D), 2 d later (E and F), and 3 d later (G and H). Note the abnormal development of PSVs in *pat2-2* mutant.

(I) to (L) Immunoblot showing the degradation of 2S albumin in control and *pat2-1* mutant over 3 d following the germination: immediately after stratification (I), 1 d later (J), 2 d later (K), and 3 d later (L).

Bars = 10 μ m in (A) to (F) and 20 μ m in (G) and (H).

(Lee et al., 2007; Sohn et al., 2007; Niihama et al., 2009); thus, its different subunits are obvious components of the subcellular trafficking machinery, but their functional characterization in plants is still lacking. The BFA-visualized endocytic trafficking defective1 (*ben1*) mutant, which shows only minor morphological defects, was also identified from a similar fluorescent marker-based screen using a treatment with the trafficking inhibitor BFA. *BEN1* encodes a previously uncharacterized GTP exchange factor on ADP-ribosylation factors component of early endosomal trafficking (Tanaka et al., 2009). These examples demonstrate the potential of fluorescent marker-based forward genetic

screens to identify previously uncharacterized components of subcellular trafficking or to place known regulators into a new functional context.

Evolutionarily Conserved AP-3 β Plays a Role in the Biogenesis and Function of the Lytic Vacuole

The function of the AP-3 complex has been addressed in various organisms, including *Dictyostelium discoideum*, *Saccharomyces cerevisiae*, *Caenorhabditis elegans*, *Drosophila melanogaster*, and mammals such as *Mus musculus* and *Homo sapiens* (Boehm and Bonifacino, 2002; Bassham et al., 2008; Dell'Angelica, 2009). These studies elucidated the role of AP-3 in vesicle-mediated trafficking to the vacuole in yeast and lysosome-related organelles in flies and mammals. In yeast, AP-3-defective mutants show abnormal delivery of vacuolar cargos, such as ALP and the vacuolar t-SNARE Vam3p but do not display any obvious morphological phenotypes (Cowles et al., 1997; Stepp et al., 1997). On the other hand, in flies and mammals, mutations in the AP-3 complex lead to defects in the function of lysosome-related organelles and causes phenotypes, such as hypopigmentation of the eyes, coat, and skin, prolonged bleeding, and lysosomal abnormalities (Dell'Angelica et al., 1999; Feng et al., 1999; Kretzschmar et al., 2000). Hence, AP-3 plays an important role in the functions of vacuole- and lysosome-related organelles in eukaryotes.

In plants, including *Arabidopsis*, the function of the AP-3 complex has so far been only poorly defined (Lee et al., 2007; Sohn et al., 2007). Nonetheless, *ap-3* μ (*zig suppressor4*) has been identified as a suppressor of the *zig1/vti11*, a mutant defective in shoot gravitropism (Kato et al., 2002; Niihama et al., 2009). As VTI11 is a regulator of vesicle trafficking between the TGN and PVC/vacuole (Surpin et al., 2003; Sanmartin et al., 2007), this suggested a role for the AP-3 complex in trafficking between post-Golgi compartments and the vacuole.

Here, we show that the putative *Arabidopsis* AP-3 β can to a large extent complement a yeast mutant defective in the AP-3 β -subunit (Cowles et al., 1997), suggesting that the function of AP-3 β is evolutionarily conserved. Our analysis of the *pat2* mutant also revealed that AP-3 β function is crucial for biogenesis, morphology, and identity of lytic vacuoles in plant cells. Interestingly, the absence of the AP-3 β function did not visibly affect the performance of PSVs as demonstrated by normal sorting and delivery of PSV cargos, but the transition between PSV and lytic vacuoles was defective. As a consequence, the lytic vacuoles preserved multiple features of the PSVs, including storage instead of degradation of multiple membrane-bound and soluble cargos in the abnormally shaped, sized, and numbered lytic vacuoles. These observations suggest that although AP-3 β is evolutionarily conserved in higher plants, it has acquired a unique function in maintaining the identity of lytic vacuoles and in regulating the transition between storage and lytic vacuoles.

To investigate the mechanism by which AP-3 β regulates vacuolar function, we analyzed its subcellular distribution. The functional AP-3 β -GFP localized predominantly in the cytosol, and the very little protein that was associated with endomembranes did not show pronounced colocalization with any of the tested markers for GA, TGN, or PVC. Furthermore, the

membrane-associated AP-3 β -GFP signal was not sensitive to BFA or wortmannin, which affect TGN/early endosomes, recycling endosomes, and GA or PVC, respectively (Geldner et al., 2001; Grebe et al., 2003; Tse et al., 2004; Haas et al., 2007; Kleine-Vehn et al., 2008a). These findings show that AP-3 β is a soluble cytoplasmic protein that does not associate with known BFA- and/or wortmannin-sensitive endomembranes. These in planta results are consistent with previous findings from *Arabidopsis* protoplasts (Lee et al., 2007; Sohn et al., 2007) that another subunit of the AP3 complex, δ adaptin, resides on a so far uncharacterized compartment. Interestingly, little of the endomembrane-associated AP-3 β -GFP signal colocalizes with SEC21, and the existence of AP-3 β -GFP signal at the periphery of the BFA compartment defined by the styryl dye FM4-64 (Figures 3H and 3I) might suggest an association of AP-3 β with Golgi endomembranes and a role of AP-3 β in post-Golgi trafficking. Colocalization of AP-3 δ with EpsinR2 and TFL1 (Lee et al., 2007; Sohn et al., 2007) that are involved in protein trafficking to the vacuole and PSV, respectively, further indicates a role of AP-3 in post-Golgi trafficking toward the vacuole.

We also showed that *pat2* is defective in the localization of a pool of PVC and vacuolar markers, including the SYP22 SNARE. Interestingly, the yeast ortholog of the *Arabidopsis* SYP22 is the vacuolar t-SNARE Vam3p that is transported to the vacuole via the ALP pathway and is mislocalized in yeast AP-3-deficient mutants (Cowles et al., 1997; Stepp et al., 1997). The yeast ALP pathway is an AP-3-mediated trafficking pathway from the late Golgi to the vacuole that bypasses the late endosomes/PVC/MVB.

The normal trafficking of cargos destined for storage or degradation to the otherwise functionally compromised *pat2* vacuoles (including abnormal vacuole morphology and mislocalization of vacuolar and/or PVC markers, such as EGFP- δ TIP, SYP22-YFP, and GFP-RABF2b) together with the localization of the AP-3 β to compartments distinct from the major known vacuolar trafficking routes suggests the existence of a previously unknown AP-3-dependent trafficking route in plant cells. This AP-3-mediated trafficking could regulate vacuolar identity and function independently from the main PVC-based cargo delivery route to the vacuole. Thus, manipulation of this vacuolar regulatory pathway could provide the means to specifically engineer the performance of the lytic vacuoles without affecting other cellular functions or overall plant development.

METHODS

Plant Material and Growth Conditions

The plant material used is listed in Supplemental Table 1 online. Seedlings were grown vertically in Petri dishes on 0.8% agar 0.5 \times Murashige and Skoog (MS) medium containing 1% sucrose, pH 5.9, at 18°C, and under long-day photoperiod unless otherwise indicated.

EMS Mutagenesis, Mutant Forward Genetic Screen, and Mapping

M2 seedlings (25,000), progenies of 1500 M1 3% EMS-mutagenized *PIN1_{pro}:PIN1-GFP* plants, were analyzed under the epifluorescence microscope for abnormal intracellular accumulation of PIN1-GFP signal. See Supplemental Methods online for details.

Cloning and *Arabidopsis thaliana* Transformation

For promoter analysis, we made a transcriptional fusion of the 1.5-kb AP-3 β promoter (amplified with primers attB1_ β 3_transl/transcr_FP and attB2_ β 3_transc_RP); for gene localization, a translational fusion of the AP-3 β genomic DNA together with the 1.5-kb promoter (amplified with primers attB1_ β 3_transl/transcr_FP and attB2_ β 3_over/transl_RP); and for overexpression, AP-3 β genomic DNA (amplified with primers attB1_ β 3_over/const_FP and attB2_ β 3_over/transl_RP) was cloned under the 35S promoter. All AP-3 β clones were amplified from genomic templates and introduced by Gateway recombination first, into pDONR221, and then into one of the destination vectors: pK7WFS7,0; pB7FWG,0; and pK7FWG2,0 (Karimi et al., 2002; <http://www.psb.ugent.be/gateway>). Primer sequences are listed in Supplemental Table 2 online.

Yeast Constructs, Transformation, and Complementation

The AP-3 β gene was amplified (using primers attB1_ β 3_over/const_FP and attB2_ β 3_const_RP) from cDNA templates and inserted by Gateway recombination first into pDONR221 and then into the yeast expression vector pAG425GPD-ccdB (*Saccharomyces cerevisiae* Advanced Gateway Destination vector from Addgene) (Alberti et al., 2007). Primer sequences are listed in Supplemental Table 2 online. SEY6210/WT (MAT α *leu 2-3*, *112 ura 3-52 his 3- Δ 200*, *trp 1- Δ 901 lys 2-801 suc 2- Δ*), CCY255/apl6 Δ , and pRS426 GFP-ALP have been described previously (Cowles et al., 1997). See Supplemental Methods online for details.

Drug Treatments and Microscopy

To assess different biological processes 5-d-old seedlings were incubated in MS medium supplemented with cycloheximide (Sigma-Aldrich; 50 μ M in DMSO), LysoTracker red (Invitrogen; 2 or 4 μ M in DMSO), BCECF (Invitrogen; 10 μ M in DMSO), BFA (Invitrogen; 50 μ M in DMSO), and wortmannin (Alexis Biochemicals; 33 μ M in DMSO). Control treatments were done in the same way with an equivalent concentration of DMSO. For FM4-64 (Invitrogen; in water) accumulation, the seedlings were pulse labeled 5 min in MS liquid medium supplemented with 2 or 4 μ M FM4-64 on ice, washed three times at room temperature in MS liquid medium, mounted, and observed at the time points indicated. For the double treatments, the seedlings were first pulse labeled with 50 μ M BFA and 2 or 4 μ M FM4-64 as described above, followed by incubation in MS medium supplemented with 50 μ M BFA.

Transmission Electron Microscopy on Roots

PIN1-GFP, wild-type, *pat2-1*, and *pat2-2* root tips of 4-d-old seedlings were excised, immersed in 20% (w/v) BSA, and frozen immediately in a high-pressure freezer (EM PACT; Leica Microsystems). Freeze substitution was performed in an EM AFS 2 (Leica Microsystems). Over a period of 4 d, root tips were freeze substituted in dry acetone as follows: -78°C for 26 h, 2°C per hour increase for 9 h, -60°C for 16 h, 2°C per hour increase for 15 h, and -30°C for 8 h. Samples were then slowly warmed up to 4°C, infiltrated stepwise over 3 d at 4°C in LR-White, hard grade (London Resin), and embedded in capsules. Polymerization was done by UV illumination for 24 h at 4°C followed by 16 h at 60°C. Ultrathin sections of gold interference color were cut with an ultramicrotome (Leica EM UC6) and collected on formvar-coated copper mesh grids. Sections were poststained in a Leica EM AC20 for 30 min in uranyl acetate at 20°C and for 7 min in lead stain at 20°C. For immunolabeling, we used anti-GFP rabbit (AbCam; 1:25). Grids were viewed with a 1010 transmission electron microscope (JEOL) operating at 80 kV.

Transmission Electron Microscopy on Seeds

PIN1-GFP, wild-type Columbia, *pat2-1*, and *pat2-2* seeds were imbibed overnight at 4°C on filter paper with deionized water after which embryos and endosperm were separated from the seed coat. The tissues were fixed by immersion in a fixative solution of 3% paraformaldehyde and 0.3% glutaraldehyde in 0.1 M Na-cacodylate buffer, pH 7.2, under vacuum for 4 h at room temperature and for 14 h at 4°C under rotation. After three washes for 2 h in 0.1 M Na-cacodylate buffer, pH 7.2, at 4°C, the samples were dehydrated through a graded ethanol series under rotation, infiltrated stepwise over 3 d at 4°C in LR-White, hard grade, and embedded in capsules. Polymerization was done by UV illumination for 1 week at 4°C followed by 1 week at room temperature. Ultrathin sections of 70 nm (gold interference color) were cut with a Leica EM UC6 ultramicrotome and collected on formvar-coated copper mesh grids. All immunolabeling steps were performed in a humid chamber at room temperature. Grids were floated upside down on 25 μ L of blocking solution (5% [w/v] BSA and 1% [w/v] fish skin gelatin [in PBS]) for 30 min followed by washing six times for 5 min each time with 1% BSA in PBS. Incubation in 1% BSA in PBS of primary antibodies for 60 min was followed by washing six times for 5 min each time with 0.1% BSA in PBS. The grids were incubated with PAG10 nm (Cell Biology) and washed twice for 5 min each time with 0.1% BSA in PBS, PBS, and deionized, distilled water. Sections were poststained for 30 min in uranyl acetate at 20°C and for 7 min in lead stain at 20°C. For immunolabeling, we used anti-2S albumin rabbit (De Clercq et al., 1990; 1:100). Grids were viewed with a 1010 transmission electron microscope (JEOL) operating at 80 kV.

Immunoblots and SDS-PAGE

Protein extracts were prepared from 10 (precursors analysis) or 15 (degradation experiment) dry seeds per each line in SDS-PAGE sample buffer and subjected to SDS-PAGE followed by either Coomassie Brilliant Blue staining or blotting to ECL membranes (GE Healthcare) as described before (Shimada et al., 2006). The membranes were treated with antibodies against 2S albumin (rabbit; 1:5000) and ECL-Anti-Rabbit IgG, horseradish peroxidase (GE Healthcare; 1:5000). The immunoreactive signals were detected using the ECL detection system (GE Healthcare).

Accession Numbers

Sequence data from this article can be found in the Arabidopsis Genome Initiative or GenBank/EMBL databases under the following accession numbers: AP-3 β (At3g55480), barley aleurain (X05167), RABF1 (At3g54840), RABF2b (AT4g19640), δ TIP (U39485), N-ST (AJ243198), PIN1 (At1g73590), PIN2 (At5G57090), PIN7 (At1g23080), PIP2a (X75883), SYP22 (U88045), VHAA1 (At2g28520), VPS29 (At3g47810), WAVE13Y/VTI12 (At1g26670), and yeast APL6/ β 3 (NP_011777).

Supplemental Data

The following materials are available in the online version of this article.

Supplemental Figure 1. *pat2* Displays Intracellular Accumulation of PM and Soluble Proteins.

Supplemental Figure 2. *pat2* Mutation Causes Enhanced Vacuolar Accumulation of Polar and Nonpolar Integral PM Proteins.

Supplemental Figure 3. *pat2* Morphological Phenotypes Remind of Mutants Defective in Vacuolar Function.

Supplemental Figure 4. PIN1-GFP Trafficking to PM, Recycling, and Early Endocytosis Are Not Affected in *pat2*.

Supplemental Figure 5. AP-3 β_{pro} :AP-3 β -GFP Complements *pat2-1* Defects.

Supplemental Figure 6. AP-3 β_{pro} :GFP-GUS Displays Ubiquitous Embryonic and Postembryonic Expression.

Supplemental Figure 7. AP-3 β -GFP Localizes to a BFA- and Wortmannin-Insensitive Compartment.

Supplemental Figure 8. *pat2* Is Not Defective in the Localization of Golgi and TGN Markers.

Supplemental Figure 9. *pat2* Shows Enhanced Vacuolar Accumulation of Integral PM Proteins and Disrupted Lytic Vacuole Morphology.

Supplemental Figure 10. *pat2* Is Defective in the Morphology, Biogenesis, and Identity of the Lytic Vacuole.

Supplemental Figure 11. *pat2* Displays Altered Morphology of PSV.

Supplemental Figure 12. The *pat2* Mutation Disrupts the Transition from PSVs to the Lytic Vacuoles.

Supplemental Figure 13. *pat2* Is Not Defective in the Degradation of Storage Proteins.

Supplemental Table 1. List of *Arabidopsis* Marker Lines, Crosses, and Constructs, and *S. cerevisiae* Strains.

Supplemental Table 2. List of Primers.

Supplemental Methods.

Supplemental References.

ACKNOWLEDGMENTS

We thank Scott D. Emr, Natasha V. Raikhel, David G. Robinson, and Alain Goossens for sharing published material; the ABRC and Nottingham Arabidopsis Stock Centre for the seed stock supply; Katerina Malinska, Rita Gross-Hardt, and Lixin Li for helpful information on different techniques; Stéphanie Robert, Niloufer Irani, Hirokazu Tanaka, Tomasz Nodzynski, Steffen Vanneste, and Zhaojun Ding for helpful discussions, suggestions, and technical assistance; Natasha V. Raikhel and Stéphanie Robert for critical reading of the manuscript; and Martine De Cock for help in preparing it. This work was supported by grants from the EMBO Young Investigator Program (to J.F.) and the Odysseus Programme of the Research Foundation-Flanders (to J.F.). J.K.-V. is indebted to the Friedrich Ebert Stiftung for a fellowship.

Received March 18, 2010; revised July 16, 2010; accepted July 23, 2010; published August 20, 2010.

REFERENCES

- Abas, L., Benjamins, R., Malenica, N., Paciorek, T., Wiśniewska, J., Moulinier-Anzola, J.C., Sieberer, T., Friml, J., and Luschnig, C. (2006). Intracellular trafficking and proteolysis of the Arabidopsis auxin-efflux facilitator PIN2 are involved in root gravitropism. *Nat. Cell Biol.* **8**: 249–256.
- Alberti, S., Gitler, A.D., and Lindquist, S. (2007). A suite of Gateway cloning vectors for high-throughput genetic analysis in *Saccharomyces cerevisiae*. *Yeast* **24**: 913–919.
- Bascham, D.C., Brandizzi, F., Otegui, M., and Sanderfoot, A.A. (2008). The secretory system of *Arabidopsis*. The Arabidopsis Book, C.R. Somerville and E.M. Meyerowitz, eds (Rockville, MD: American Society of Plant Biologists), doi/10.1199/tab.0116, <http://www.aspb.org/publications/arabidopsis/>.
- Benková, E., Michniewicz, M., Sauer, M., Teichmann, T., Seifertová, D., Jürgens, G., and Friml, J. (2003). Local, efflux-dependent auxin

- gradients as a common module for plant organ formation. *Cell* **115**: 591–602.
- Bilou, I., Xu, J., Wildwater, M., Willemsen, V., Paponov, I., Friml, J., Heidstra, R., Aida, M., Palme, K., and Scheres, B.** (2005). The PIN auxin efflux facilitator network controls growth and patterning in *Arabidopsis* roots. *Nature* **433**: 39–44.
- Boehm, M., and Bonifacio, J.S.** (2002). Genetic analyses of adaptin function from yeast to mammals. *Gene* **286**: 175–186.
- Cowles, C.R., Odorizzi, G., Payne, G.S., and Emr, S.D.** (1997). The AP-3 adaptor complex is essential for cargo-selective transport to the yeast vacuole. *Cell* **91**: 109–118.
- Cutler, S.R., Ehrhardt, D.W., Griffiths, J.S., and Somerville, C.R.** (2000). Random GFP, cDNA fusions enable visualization of subcellular structures in cells of *Arabidopsis* at a high frequency. *Proc. Natl. Acad. Sci. USA* **97**: 3718–3723.
- De Clercq, A., Vandewiele, M., De Ryke, R., Van Damme, J., Van Montagu, M., Krebbers, E., and Vandekerckhove, J.** (1990). Expression and processing of an *Arabidopsis* 2S albumin in transgenic tobacco. *Plant Physiol.* **92**: 899–907.
- Dell'Angelica, E.C.** (2009). AP-3 dependent trafficking and disease: The first decade. *Curr. Opin. Cell Biol.* **21**: 552–559.
- Dell'Angelica, E.C., Shotelersuk, V., Aquilar, R.C., Gahl, W.A., and Bonifacio, J.S.** (1999). Altered trafficking of lysosomal proteins in Hermansky-Pudlak Syndrome due to mutations in the β 3A subunit of the AP-3 adaptor. *Mol. Cell* **3**: 11–21.
- Dettmer, J., Hong-Hermesdorf, A., Stierhof, Y.-D., and Schumacher, K.** (2006). Vacuolar H⁺-ATPase activity is required for endocytic and secretory trafficking in *Arabidopsis*. *Plant Cell* **18**: 715–730.
- Dhonukshe, P., Aniento, F., Hwang, I., Robinson, D.G., Mravec, J., Stierhof, Y.-D., and Friml, J.** (2007). Clathrin-mediated constitutive endocytosis of PIN auxin efflux carriers in *Arabidopsis*. *Curr. Biol.* **17**: 520–527.
- Dhonukshe, P., et al.** (2008). Generation of cell polarity in plants links endocytosis, auxin distribution and cell fate decisions. *Nature* **456**: 962–966.
- di Sansebastiano, G.P., Paris, N., Marc-Martin, S., and Neuhaus, J.M.** (2001). Regeneration of a lytic central vacuole and of neutral peripheral vacuoles can be visualized by green fluorescent proteins targeted to either type of vacuoles. *Plant Physiol.* **126**: 78–86.
- Ebine, K., Okatani, Y., Uemura, T., Goh, T., Shoda, K., Niihama, M., Morita, M.T., Spitzer, C., Otegui, M.S., Nakano, A., and Ueda, T.** (2008). SNARE complex unique to seed plants is required for protein storage vacuole biogenesis and seed development of *Arabidopsis thaliana*. *Plant Cell* **20**: 3006–3021.
- Feng, L., Seymour, A.B., Jiang, S., To, A., Peden, A.A., Novak, E.K., Zhen, L., Rusiniak, M.E., Eicher, E.M., Robinson, M.S., Gorin, M.B., and Swank, R.T.** (1999). The beta3A subunit gene (Ap3b1) of the AP-3 adaptor complex is altered in the mouse hypopigmentation mutant pearl, a model for Hermansky-Pudlak syndrome and night blindness. *Hum. Mol. Genet.* **8**: 323–330.
- Frigerio, L., Hinz, G., and Robinson, D.G.** (2008). Multiple vacuoles in plant cells: Rule or exception? *Traffic* **9**: 1564–1570.
- Geldner, N., Dénervaud-Tendon, V., Hyman, D.L., Mayer, U., Stierhof, Y.D., and Chory, J.** (2009). Rapid, combinatorial analysis of membrane compartments in intact plants with a multicolor marker set. *Plant J.* **59**: 169–178.
- Geldner, N., Friml, J., Stierhof, Y.-D., Jürgens, G., and Palme, K.** (2001). Auxin transport inhibitors block PIN1 cycling and vesicle trafficking. *Nature* **413**: 425–428.
- Gebe, M., Xu, J., Möbius, W., Ueda, T., Nakano, A., Geuze, H.J., Rook, M.B., and Scheres, B.** (2003). *Arabidopsis* sterol endocytosis involves actin-mediated trafficking via ARA6-positive early endosomes. *Curr. Biol.* **13**: 1378–1387.
- Haas, T.J., Sliwinski, M.K., Martinez, D.E., Preuss, M., Ebine, K., Ueda, T., Nielsen, E., Odorizzi, G., and Otegui, M.S.** (2007). The *Arabidopsis* AAA ATPase SKD1 is involved in multivesicular endosome function and interacts with its positive regulator LYST-INTERACTING PROTEIN5. *Plant Cell* **19**: 1295–1312.
- Jaillais, Y., Fobis-Loisy, I., Miège, C., Rollin, C., and Gaude, T.** (2006). AtSNX1 defines an endosome for auxin-carrier trafficking in *Arabidopsis*. *Nature* **443**: 106–109.
- Karimi, M., Inzé, D., and Depicker, A.** (2002). GATEWAY vectors for *Agrobacterium*-mediated plant transformation. *Trends Plant Sci.* **7**: 193–195.
- Kato, T., Morita, M.T., Fukaki, H., Yamauchi, Y., Uehara, M., Niihama, M., and Tasaka, M.** (2002). SGR2, a phospholipase-like protein, and ZIG/SGR4, a SNARE, are involved in the shoot gravitropism of *Arabidopsis*. *Plant Cell* **14**: 33–46.
- Kleine-Vehn, J., Dhonukshe, P., Sauer, M., Brewer, P.B., Wiśniewska, J., Paciorek, T., Benková, E., and Friml, J.** (2008a). ARF GEF-dependent transcytosis and polar delivery of PIN auxin carriers in *Arabidopsis*. *Curr. Biol.* **18**: 526–531.
- Kleine-Vehn, J., Leitner, J., Zwiewka, M., Sauer, M., Abas, L., Luschning, C., and Friml, J.** (2008b). Differential degradation of PIN2 auxin efflux carrier by retromer-dependent vacuolar targeting. *Proc. Natl. Acad. Sci. USA* **105**: 17812–17817.
- Kretschmar, D., Poeck, B., Roth, H., Ernst, R., Keller, A., Porsch, M., Strauss, R., and Pflugfelder, G.O.** (2000). Defective pigment granule biogenesis and aberrant behavior caused by mutations in the *Drosophila* AP-3b adaptin gene *ruby*. *Genetics* **155**: 213–223.
- Laxmi, A., Pan, J., Morsy, M., and Chen, R.** (2008). Light plays an essential role in intracellular distribution of auxin efflux carrier PIN2 in *Arabidopsis thaliana*. *PLOS One* **3**: e1510.
- Lee, G.-J., Kim, H., Kang, H., Jang, M., Lee, D.W., Lee, S., and Hwang, I.** (2007). EpsinR2 interacts with clathrin, Adaptor Protein-3, AtVTI12, and phosphatidylinositol-3-phosphate. Implications for EpsinR2 function in protein trafficking in plant cells. *Plant Physiol.* **143**: 1561–1575.
- Marty, F.** (1999). Plant vacuoles. *Plant Cell* **11**: 587–599.
- Niihama, M., Takemoto, N., Hashiguchi, Y., Tasaka, M., and Morita, M.T.** (2009). ZIP genes encode proteins involved in membrane trafficking of the TGN-PVC/vacuoles. *Plant Cell Physiol.* **50**: 2057–2068.
- Petrásek, J., et al.** (2006). PIN proteins perform a rate-limiting function in cellular auxin efflux. *Science* **312**: 914–918.
- Robert, S., Chary, S.N., Drakakaki, D., Li, S., Yang, Z., Raikhel, N.V., and Hicks, G.R.** (2008). Endosidin1 defines a compartment involved in endocytosis of the brassinosteroid receptor BRI1 and the auxin transporters PIN2 and AUX1. *Proc. Natl. Acad. Sci. USA* **105**: 8464–8469.
- Robinson, D.G., Jiang, L., and Schumacher, K.** (2008). The endosomal system of plants: Charting new and familiar territories. *Plant Physiol.* **147**: 1482–1492.
- Rojo, E., Gillmor, C.S., Kovaleva, V., Somerville, C.R., and Raikhel, N.V.** (2001). VACUOLELESS1 is an essential gene required for vacuole formation and morphogenesis in *Arabidopsis*. *Dev. Cell* **1**: 303–310.
- Sanmartín, M., Ordonez, A., Sohn, E.J., Robert, S., Sanchez-Serrano, J.J., Surpin, M.A., Raikhel, N.V., and Rojo, E.** (2007). Divergent functions of VTI12 and VTI11 in trafficking to storage and lytic vacuoles in *Arabidopsis*. *Proc. Natl. Acad. Sci. USA* **104**: 3645–3650.
- Shimada, T., Koumoto, Y., Li, L., Yamazaki, M., Kondo, M., Nishimura, M., and Hara-Nishimura, I.** (2006). AtVPS29, a putative component of a retromer complex, is required for the efficient sorting of seed storage proteins. *Plant Cell Physiol.* **47**: 1187–1194.
- Silady, R.A., Ehrhardt, D.W., Jackson, K., Faulkner, C., Oparka, K., and Somerville, C.R.** (2008). The GRV2/RME-8 protein of *Arabidopsis*

- functions in the late endocytic pathway and is required for vacuolar membrane flow. *Plant J.* **53**: 29–41.
- Sohn, E.J., Rojas-Pierce, M., Pan, S., Carter, C., Serrano-Mislata, A., Madueno, F., Rojo, E., Surpin, M., and Raikhel, N.V.** (2007). The shoot meristem identity gene TFL1 is involved in flower development and trafficking to the protein storage vacuole. *Proc. Natl. Acad. Sci. USA* **104**: 18801–18806.
- Stepp, J.D., Huang, K., and Lemmon, S.K.** (1997). The yeast adaptor protein complex, AP-3, is essential for the efficient delivery of alkaline phosphatase by the alternate pathway to the vacuole. *J. Cell Biol.* **139**: 1761–1774.
- Surpin, M., Zheng, H., Morita, M.T., Saito, C., Avila, E., Blakeslee, J.J., Bandyopadhyay, A., Kovaleva, V., Carter, D., Murphy, A., Tasaka, M., and Raikhel, N.** (2003). The VTI family of SNARE proteins is necessary for plant viability and mediates different protein transport pathways. *Plant Cell* **15**: 2885–2899.
- Swanson, S.J., and Jones, R.L.** (1996). Gibberellic acid Induces vacuolar acidification in barley aleurone. *Plant Cell* **8**: 2211–2221.
- Tamura, K., Shimada, T., Ono, E., Tanaka, Y., Nagatani, A., Higashi, S.I., Watanabe, M., Nishimura, M., and Hara-Nishimura, I.** (2003). Why green fluorescent fusion proteins have not been observed in the vacuoles of higher plants. *Plant J.* **35**: 545–555.
- Tanaka, H., Kitakura, S., De Rycke, R., De Groodt, R., and Friml, J.** (2009). Fluorescence imaging-based screen identifies ARF GEF component of early endosomal trafficking. *Curr. Biol.* **19**: 391–397.
- Tse, Y.C., Mo, B., Hillmer, S., Zhao, M., Lo, S.W., Robinson, D.G., and Jiang, L.** (2004). Identification of multivesicular bodies as prevacuolar compartments in *Nicotiana tabacum* BY-2 cells. *Plant Cell* **16**: 672–693.
- Ueda, T., Yamaguchi, M., Uchimiya, H., and Nakano, A.** (2001). Ara6, a plant-unique novel type Rab GTPase, functions in the endocytic pathway of *Arabidopsis thaliana*. *EMBO J.* **20**: 4730–4741.
- Wiśniewska, J., Xu, J., Seifertova, D., Brewer, P.B., Ruzicka, K., Bilou, I., Rouquie, D., Benkova, E., Scheres, B., and Friml, J.** (2006). Polar PIN localization directs auxin flow in plants. *Science* **312**: 883.
- Xu, J., and Scheres, B.** (2005). Dissection of *Arabidopsis* ADP-RIBOSYLATION FACTOR 1 function in epidermal cell polarity. *Plant Cell* **17**: 525–536.
- Yamazaki, M., Shimada, T., Takahashi, H., Tamura, K., Kondo, M., Nishimura, M., and Hara-Nishimura, I.** (2008). Arabidopsis VPS35, a retromer component, is required for vacuolar protein sorting and involved in plant growth and leaf senescence. *Plant Cell Physiol.* **49**: 142–156.